Penerbit Akademia Baru

Journal of Advanced Research in Fluid Mechanics and Thermal Sciences

Journal homepage: www.akademiabaru.com/arfmts.html
ISSN: 2289-7879

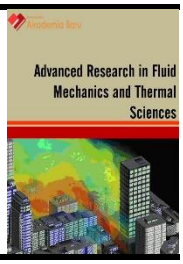

Evaluating the GMAW Joint with a Constant Heat Input

Open Access

Djarot B. Darmadi[1,*], Lingga P. Setiawan[1], Shahruddin Mahzan[2]

[1] Department of Mechanical Engineering, Brawijaya University, Malang – 65145, Indonesia
[2] Department of Mechanical Engineering, University Tun Hussein Onn, Malaysia

ARTICLE INFO

Article history:
Received 2 October 2018
Received in revised form 27 December 2018
Accepted 30 December 2018
Available online 12 February 2019

ABSTRACT

The most important aspect of the overall welding process is determining the welding parameters which are usually described in a form of *Welding Procedure Specification – WPS.* WPS is written by an experienced welding engineer. Following the WPS in the welding application is expected to provide optimum joint properties for a certain applied load and environment conditions. One of the most important parameter which is frequently prescribed in WPS is heat input. This paper is presented based on the curiosity to prove the equal heat input does not always produce identical joint. An actual experiment method of constant heat input welding was implemented by varying welding speed with adjusted electric current. The tensile test then is carried out to the weldments to analyze the effect of the varied welding parameters. Finite Element Method (FEM) was used to acuminate the analysis. Using the FEM the temperature history of desired position can be obtained. This temperature history is an important additional data to give a technical reason why the tensile strength is as what exhibited by data from tensile test. The tensile test shows that with higher electric current the higher tensile strength is obtained. From temperature history, which is emulated by FEM, the higher electric current originates faster cooling rate. This faster cooling rate produces harder joint and in turn provides higher tensile strength which is confirmed by the tensile test.

Keywords:
Heat input, welding, welding speed, electric current

1. Introduction

Previously welding was considered as a craft rather than a science. After technology for welding machine is advance developed using closed-loop-in-process control combined with automation, welding process becomes a scientific knowledge which is reproducible [1,2]. For such automated process the suitable selection of welding parameters determines the quality of resulted joint [3,4]. Sriintharasut *et al.,* [5] evaluated two types of welding current on the nickel-aluminum-bronze (NAB) joints [5]. The results show that pulsed current is suitable for groove welding due to its deeper penetration and higher dilution ratio, while standard current is appropriate for built-up overlay welding. Zhou *et al.,* [6] observed the effect of welding speed to dissimilar welded joint of aluminum

*Corresponding author.
E-mail address: b_darmadi_djarot@ub.ac.id (Djarot B. Darmadi)

and brass. The optimum speed is 0.5-0.6 m/min which provides joint without obvious defect. Beyond the range the welding produces excessive back reinforcement and cracking. The maximum tensile strength was obtained for the 0.5 m/min provides welding efficiency 55.7% of Al base metal. MN Ayof *et al.,* [7] studied the effect of parameters such as arc voltage on the welding joint of SS304 and BS1387 steels. For a high voltage (21.5 Volt) the increasing current increases the tensile strength while the reverse is shown by a low voltage (17.0 Volt). Mohd Shoeb *et al.,* [8] discussed the effects of gas flow rate to the weld bead profile. It is found that the gas flow rate has no effect on penetration and width, but at the height of the weld bead. In certain gas flow rate, increasing arc voltage decreases the high of the weld bead in which this declining is more significant for a lower gas flow rate.

In practice the welding parameters are prescribed by experienced welding engineers, which are written in the Welding Procedure Specification (WPS) form. One of the parameters which is often defined in WPS is heat input [9-12]. It is assumed that with a specific heat input certain quality of joint will be obtained, since heat input is defined as the heat provides by a welding torch for a certain weld length. Thus, for a defined length of weld joint a certain amount of heat is embedded in the weld metal for a denominated heat input. In this article the heat input is maintained to be constant while the inputted heat and welding speed were varied. The heat is varied by altering electric current while voltage is fixed. The electric current must be properly adjusted to obtain equal heat input.

2. Methodology

This research used actual experimental method approach by evaluating the quality of resulted joint which is represented by the tensile strength of the weld joint. The independent variables are electric current and welding speed. Their combination is maintained to obtain equal heat input. The dependent variables are tensile strength of the joint. The GMAW ESAB Compact 250 welding machine as shown in Figure 1 was used. The electric power was maintained by keeping the voltage equal to 19 Volt. The shielding gas was the CO_2 with debit equal to 20 liters/minute. The AWS: ER70S-6 consumable electrode with diameter equal to 0.8mm was used as a filler metal. This electrode was fed with feed rate equal to 2,5m/min which means around 21 mm^3 of filler metal is embedded to form a weld joint. The type of shielding gas and wire were chosen following Table 1.

Fig. 1. The ESAB Compact 250 GMAW machine

Table 1
The suitable wire and shielding gas [13]

Type of steel(1)	Trade design.(2)	JIS classification(3)	AWS classification(3)	Typical shielding gas	Welding position(4)
490HT	MG-50	Z3312 YGW11	A5.18 ER70S-G	CO_2	F, H, HF
	MG-51T	Z3312 YGW12	A5.18 ER70S-6	CO_2	All position
	MG-S50	Z3312 G49AP3M 16	A5.18 ER70S-G	80%Ar+20%CO_2	All position
	DW-100	Z3313 T49J0T1-1CA-U	A5.20 E71T-1C	CO_2	All position
	MX-100	Z3313 T49J0T 15-0CA-U	A5.20 E70T-1C	CO_2	F, H, HF
590HT	MG-60	Z3312 G59JA1UC 3M1T	A5.28 ER80S-G	CO_2	All position
	MG-S63B	Z3312 G59JA1UMC1M1T	A5.28 ER90S-G	80%Ar+20%CO_2	All position
690HT	MG-S70	Z3312 G69A2UM N4CM21T	A5.28 ER100S-G	80%Ar+20%CO_2	All position
780HT	MG-S80	Z3312 G78A4M N5CM3T	A5.28 ER110S-G	80%Ar+20%CO_2	All position

Note: (1) Classified by tensile strength (MPa)
(2) Trade designations of wires produced by Kobe Steel
(3) As per JIS Z3312:2009, JIS Z3313:2009, AWS A5. 18:2005, A5.20:2005, and A5.28:2005
(4) F: flat, H: horizontal, HF: horizontal fillet.

The heat input was kept around 5100 J/mm. The electric current and welding speed were altered by adjusting the current setting in welding machine and longitudinal travelling velocity respectively. The actual current also measured using ampere meter at the inputting power wire. The welding speed was regulated using an automatic robot as shown in Figure 2. Two 5 mm plates with 400mm and 200mm were joined in the middle at 400mm side to form a 400mm x 400mm square. Single V surface preparation with 60° trimmed edges following AS 2885.2 standard was formed on the joint surfaces before welded.

Fig. 2. The mechanism to control welding speed

The plate was hypo-eutectoid steel with 0.15% C. The composition of the steel is as shown in Table 2. To fill the V-grove two layers of weld beads were applied. The measured variations of electric current and welding speed were 89, 113, 134, 156 and 180 Amperes for welding speed equal to 1.2, 1.5, 1.8, 2.1 and 2.4 m/hour respectively. The complete installation is shown in Figure 3.

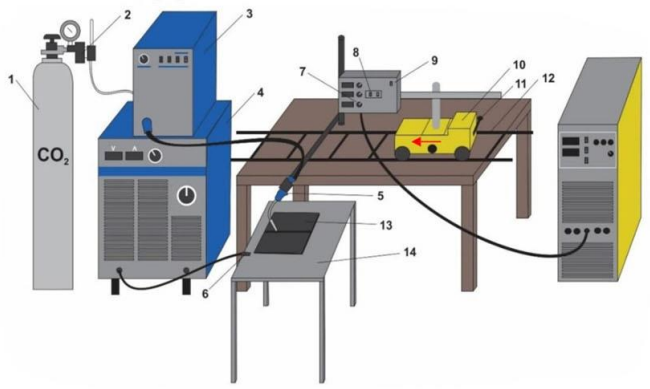

1. CO_2 tube
2. Regulator
3. Wire feed controller
4. SMAW welding machine
5. Control Unit
6. Cathode
7. Speed radio button
8. Forward or backward button
9. Welding speed panel
10. Welding speed robot
11. Locking lever
12. Welding track
13. Welded plate
14. Workbench

Fig. 3. The sketch of overall experiment set up

Table 2
The chemical composition of the steel

	C	Si	Mn	P	S	Cu	Cr	Mo	Al	Ti	N	CE
%	0.15	0.242	0.73	0.012	0.0069	0.01	0.02	0.001	0.04	0.001	0.00027	0.28

3. Results and Discussion

After welding had been applied, the tensile test was formed according to ASTM E-8 standard. The tensile test result is shown in Table 3 and Figure 4. The tabulated values were the real time data which have been obtained from measurements. It can be checked that the heat input values, although is not exactly equal to but they were around 5100 J/mm with standard deviation was ± 50 J/mm (~1% of pertained 5100 J/mm which is acceptable). From Table 1 and Figure 4, it can be said that increasing welding current generally produces stronger tensile strength. The lowest mean tensile strength is for 89 Ampere, which is equal to 306.11 N/mm^2 whilst the highest is for 180A that produces a tensile strength equal to 460 N/mm^2.

Table 3
The tensile strength obtained from tensile test

I (A)	v (m/h)	σ_u (N/mm^2)	mean (N/mm^2)
89.00	1.20	313.70 303.82 300.82	306.11
113.00	1.50	421.80 417.78 419.52	419.70
134.00	1.80	439.68 441.26 457.17	446.04
156.00	2.10	454.50 440.79 464.50	453.26
180.00	2.40	466.89 471.37 441.80	460.02

The tensile strength for 89 Ampere is too low and the provided power cannot produce good metal transfer, which in turn produces poor weld bead. The fracture of tensile test also confirms the lack of the electric power. All specimens failed at Heat Affected Zone (HAZ), except for the specimen of

89 A. Figure 5 shows the fracture surface of the 89A specimen which shown the voids on the fracture surface. Certainly, these voids notably decrease the tensile strength. Due to the existence of these voids the 89A specimen has extreme lower tensile strength and failed at the weld metal.

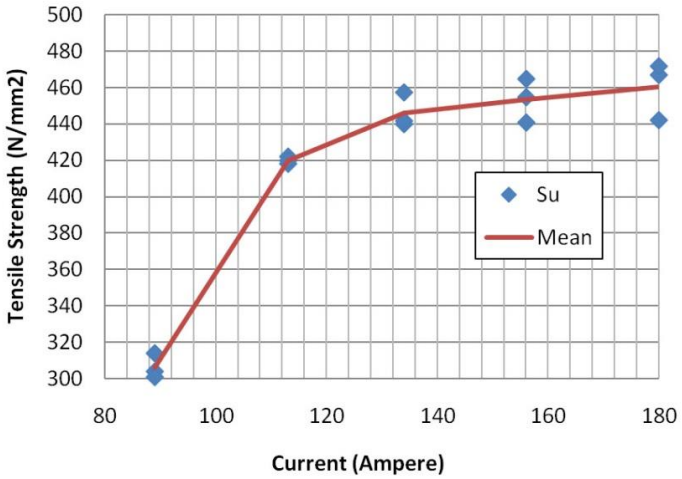

Fig. 4. The tensile strength for varied electric current

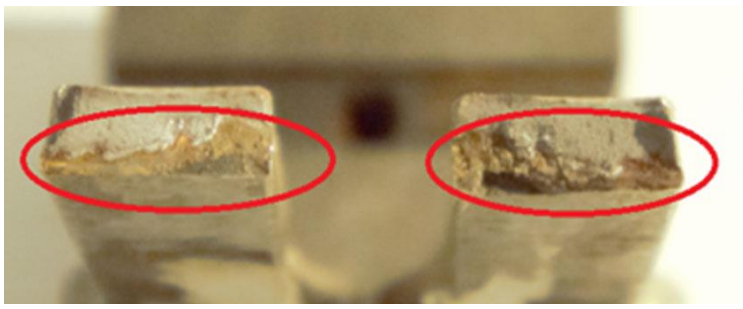

Fig. 5. Fracture surface of the 89A specimen

Specimens with electric current equal to 113, 134, 156 and 180 Amperes have good weld bead and the tensile specimens broke at HAZ, since the ultimate tensile strength of filler metal is higher compared to the base metal. The variation of HAZ tensile strength is caused by different temperature histories experienced by the HAZ. The temperature histories describe a thermal circle which is experienced by certain node (position). It is comprised of heating and cooling stages. The most important parts of the thermal cycle are peak temperature and cooling rate which both determine the developed microstructure which in turn determine the strength of HAZ. In this article the thermal cycles are obtained from validated FEM simulation [14,15].

In Figure 6 are shown thermal cycles experienced by certain nodes for specimen 180A and Figure 7 describes thermal cycles for node 4169 with varied Amperes. The transverse distance from the weld line of nodes n4168, n4169 and n4170 are 7.19, 11.7 and 16.9 millimeters respectively. Some phenomena can be retrieved from these thermal cycles. As can be seen in Figure 6, the peak temperatures from the higher to lower are n4168, n4169 and n4170 respectively since n4168 is the closest to the weld line and the n4170 is the farthest and since the heat source is travelling along weld line that is why the closer the higher the peak temperature will be. From Figure 7 which observes thermal cycles for varied amperes at node 4169, it can be said that the peak temperatures are achieved sooner for higher ampere since the higher ampere means higher welding speed to obtain equal heat input. The high welding speed means the heat source needs shorter time to achieve

an equal longitudinal position as node 4169 when the peak temperature almost come to the peak temperature.

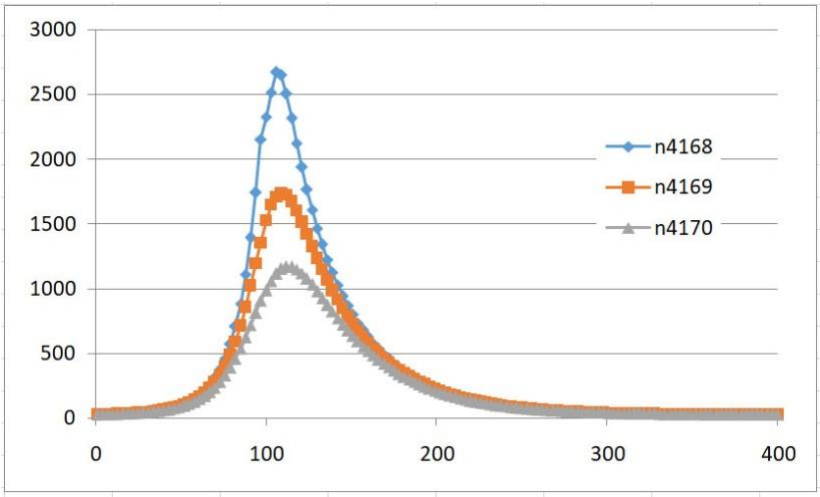

Fig. 6. Thermal cycle of 180 A for varied nodes

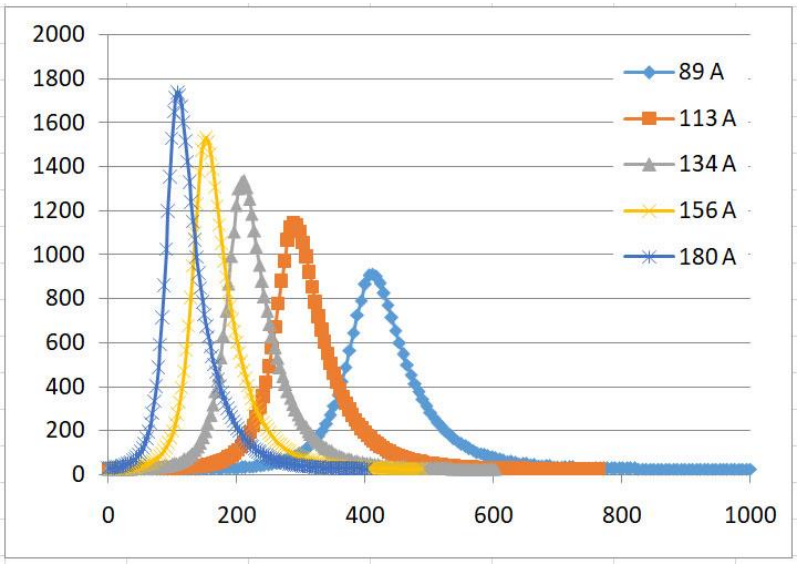

Fig. 7. Thermal cycles at node 4169 for varied amperes

Not only come early, but also with higher current the peak temperature is proportional to the current which means with higher current node 4169 has a higher peak temperature. Evaluating the peak temperature of nodes the area of Heat Affected Zone can be identified. HAZ can be determined by evaluating the experienced peak temperature. If the peak temperature of the thermal cycle for an observed node exceeds the recrystallization temperature (723 °C) this node is at HAZ. Evaluating the temperature history of nodes for different transverse distance and applying interpolation or extrapolation, it can be determined that the HAZ for 113, 134, 156 and 180 Amperes are 1.47, 1.74, 1.95, 2.11 and 2.65 cm respectively or in short it can be said higher ampere increases the width of HAZ.

The important aspect that determines the mechanical properties of a welded joint is the cooling rate. In Figure 8 shows the cooling rate of node 4169. Y axis is temperature and the X axis is time in log scale. For steel welding the most important cooling rate is cooling from 800°C to 500°C which is usually called as t8/5. It can be said from Figure 8 that the higher current results in a faster cooling

rate. The faster cooling rate produces harder microstructure which in turn increases the ultimate tensile strength. Based on the cooling rate, it can be explained the tensile strength from the highest are 180A, 156A, 134A and 115A specimens respectively. It should be noted that all the 180A, 156A, 134A and 115A produce good weld bead and the different strength is caused by different experienced thermal cycle in HAZ that is different peak temperature and cooling rates. Whilst for the 89A specimen the difference in resulted ultimate strength, not only produce by different thermal cycle, but also the current which is too low that cannot produce perfect weld bead. That is why this specimen shows extreme lowest ultimate tensile strength.

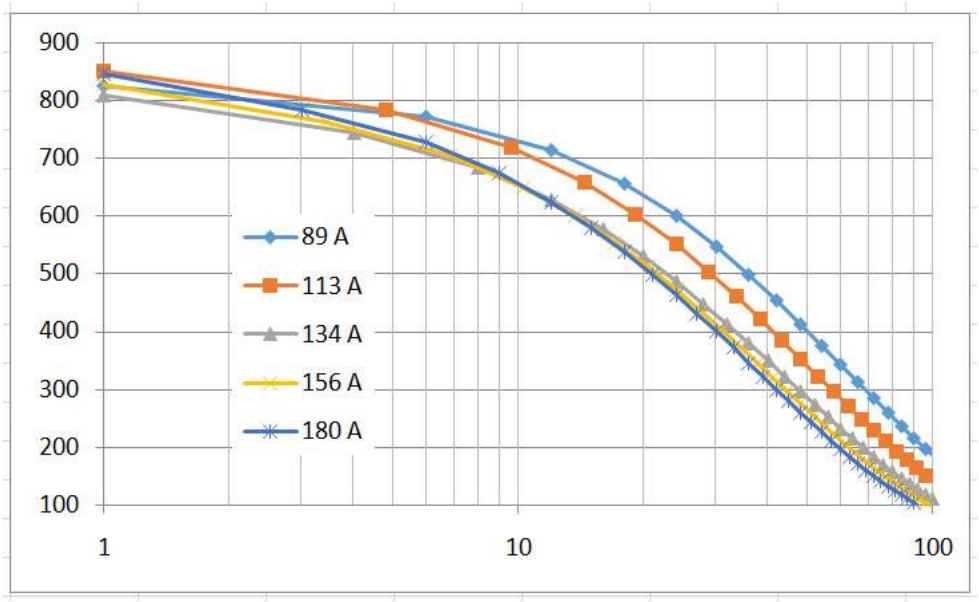

Fig. 8. Cooling rates of node 4169 for varied amperes

4. Conclusions

Based on the obtained results and analysis as discussed in section three, some important phenomenon can be resumed. First of all, it is clear that the constant heat input does not provide equal weld joint. For constant heat input, the electric current should exceed a minimum value to provide good weld bead unless void will exist. For the sufficient electric current, the tensile strength of the constant heat input with higher electric current increases due to the higher peak temperature, wider HAZ and faster cooling. This higher cooling rate produces harder HAZ which in turn produce higher ultimate strength.

References

[1] Norrish, John. *Advanced welding processes*. Elsevier, 2006.

[2] Darmadi, Djarot B. "Evaluation of the effects of melting phenomenon on the residual stress formation in ferritic pipeline multi pass girth-weld joints." *International Journal of Engineering Systems Modelling and Simulation* 8, no. 3 (2016): 205-217.

[3] Wang, Q., D. L. Sun, Y. Na, Y. Zhou, X. L. Han, and J. Wang. "Effects of TIG welding parameters on morphology and mechanical properties of welded joint of Ni-base superalloy." *Procedia Engineering* 10 (2011): 37-41.

[4] Russo Spena, Pasquale, Stefano Rossi, and Rudi Wurzer. "Effects of Welding Parameters on Strength and Corrosion Behavior of Dissimilar Galvanized Q&P and TRIP Spot Welds." *Metals* 7, no. 12 (2017): 534.

[5] Sriintharasut, Suttipong, Bovornchok Poopat, and Isaratat Phung-on. "The effects of different types of welding current on the characteristics of nickel aluminum bronze using gas metal arc welding." *Materials Today: Proceedings* 5, no. 3 (2018): 9535-9542.

[6] Zhou, L., L. Y. Luo, C. W. Tan, Z. Y. Li, X. G. Song, H. Y. Zhao, Y. X. Huang, and J. C. Feng. "Effect of welding speed on microstructural evolution and mechanical properties of laser welded-brazed Al/brass dissimilar joints." *Optics & Laser Technology* 98 (2018): 234-246.

[7] Ayof, M. N., N. I. S. Hussein, and MZ Mohd Noh. "Gas Metal Arc Welding Parameters Effect on Properties of Tailored Orbital Weld of SS304 and BS1387." In *IOP Conference Series: Materials Science and Engineering*, vol. 238, no. 1, p. 012015. IOP Publishing, 2017.

[8] Shoeb, M. O. H. D., M. Parvez, and P. Kumari. "Effect of MIG welding input process parameters on weld bead geometry on HSLA steel." *Int. J. Eng. Sci. Technol* 5, no. 1 (2013): 200-212.

[9] Melfi, Teresa. "New code requirements for calculating heat input." *welding Journal* 6 (2010).

[10] Xu, Longyun, Jian Yang, Ruizhi Wang, Wanlin Wang, and Zhongmin Ren. "Effect of Welding Heat Input on Microstructure and Toughness of Heated-Affected Zone in Steel Plate with Mg Deoxidation." *steel research international*88, no. 12 (2017): 1700157.

[11] Gupta, Aman, Amit Kumar, T. Baskaran, Shashi Bhushan Arya, and Rajesh Kisni Khatirkar. "Effect of Heat Input on Microstructure and Corrosion Behavior of Duplex Stainless Steel Shielded Metal Arc Welds." *Transactions of the Indian Institute of Metals* (2018): 1-12.

[12] Bexiga, M., A. Tavares, F. Melo, and A. Loureiro. "Effect of heat input on microstructure and strength of welds in tantalum and niobium alloys." *Ciência & Tecnologia dos Materiais* 29, no. 1 (2017): e51-e55.

[13] Kobelco. *Arc Welding of Specific Steels and Cast Iron.* Kobe Steel, LTD. Japan (2015).

[14] Darmadi, Djarot B. "PREDICTING TEMPERATURE PROFILE AND TEMPERATURE HISTORY FOR VARIED PARAMETERS OF A WELDING PROCESS USING ROSENTHAL'S APPROACH FOR SEMI-INFINITE SOLID." (2006).

[15] Lostado Lorza, Rubén, Rubén Escribano García, Roberto Fernandez Martinez, and María Ángeles Martínez Calvo. "Using Genetic Algorithms with Multi-Objective Optimization to Adjust Finite Element Models of Welded Joints." *Metals* 8, no. 4 (2018): 230.